arXiv:1604.01671v1 [astro-ph.SR] 6 Apr 2016

Rotating Stars and the Formation of Bipolar Planetary Nebulae II: Tidal Spin-up

G. García-Segura

Instituto de Astronomía, Universidad Nacional Autónoma de Mexico, Km. 103 Carr. Tijuana-Ensenada, 22860, Ensenada, B. C., Mexico

ggs@astrosen.unam.mx

E. Villaver

Departamento de Física Teórica, Universidad Autónoma de Madrid, Cantoblanco, E-28049 Madrid, Spain

A. Manchado[1,2]

Instituto de Astrofísica de Canarias, Via Láctea s/n, E-38200 La Laguna, Tenerife, Spain

N. Langer

Argelander-Institut für Astronomie, Universität Bonn, D-53121 Bonn, Germany

S.-C. Yoon

Astronomy Program, Department of Physics and Astronomy, Seoul National University, Seoul, 151-747, Republic of Korea

Received _____; accepted _____

[1]Departamento de Astrofísica, Universidad de La Laguna, E-38206 La Laguna, Tenerife, Spain

[2]Consejo Superior de Investigaciones Científicas (CSIC), Spain

ABSTRACT

We present new binary stellar evolution models that include the effects of tidal forces, rotation, and magnetic torques with the goal of testing Planetary Nebulae (PNe) shaping via binary interaction. We explore whether tidal interaction with a companion can spin up the AGB envelope. To do so we have selected binary systems with main sequence masses of 2.5 $M_\odot$ and of 0.8 $M_\odot$ and evolve them allowing initial separations of 5, 6, 7, and 8 AU. The binary stellar evolution models have been computed all the way to the PNe formation phase or until Roche lobe overflow (RLOF) is reached, whatever happens first. We show that with initial separations of 7 and 8 AU, the binary avoids entering into RLOF, and the AGB star reaches moderate rotational velocities at the surface ($\sim$ 3.5 and $\sim$ 2 km s^{-1} respectively) during the inter-pulse phases, but after the thermal pulses it drops to a final rotational velocity of only $\sim$ 0.03 km s^{-1} . For the closest binary separations explored, 5 and 6 AU, the AGB star reaches rotational velocities of $\sim$ 6 and $\sim$ 4 km s^{-1} respectively when the RLOF is initiated. We conclude that the detached binary models that avoid entering the RLOF phase during the AGB will not shape bipolar PNe, since the acquired angular momentum is lost via the wind during the last two thermal pulses. This study rules out tidal spin-up in non-contact binaries as a sufficient condition to form bipolar PNe.

Subject headings: Stars: Evolution —Stars: Rotation —Stars: Magnetic Fields —Stars: AGB and post-AGB —(Stars:) binaries: general —(ISM:) planetary nebulae: general

1. INTRODUCTION

During nearly 30 years of research in the formation of planetary nebulae (PNe), several explanations have been proposed in the literature to produce the bipolar shapes. The most popular one involves the presence of a dense medium in the equatorial latitude, which collimates the later fast stellar wind (Calvet & Peimbert 1983; Balick 1987; Icke 1988; Icke et al. 1989; Mellema 1991; Frank & Mellema 1994). A number of models, have the focus on how to form a dense medium along the equator of the asymptotic giant brach (AGB) star by stellar rotation (Ignace et al. 1996; García-Segura 1997; García-Segura et al.1999), while others concentrate on magnetic forces, succeeding only sometimes at creating such a dense medium (Matt et al. 2000).

A long debate regarding the need of a binary companion has also been taking place during these last three decades, since AGB wind asphericities could naturally arise from the interaction of AGB stars with a companion in several ways. The most popular ones involve common envelope evolution and the initial phase of spiral-in (Livio 1993; Soker 1997; Sandquist et al. 1998; Nordhaus & Blackman 2006; de Marco 2009; Ricker & Taam 2012; de Marco et al. 2013), gravitational focusing (Gawryszcak et al. 2002), wind-capture disks (Huarte-Espinosa et al. 2013) and Wind-Roche-Lobe-Overflows (Podsiadlowski & Mohamed 2007; Mohamed & Podsiadlowski 2012) . Along these lines, in our paper I (García-Segura et al. 2014) we provided a solid probe that bipolar PNe formation cannot result from the evolution of a single AGB star, given that these stars do not carry the necessary angular momentum, or to be more specific, the necessary surface rotation.

In this second paper, we explore the alternative of binary (versus single) evolution for bipolar PNe formation from the view point of stellar evolution models. We calculate the effects that a secondary star has onto the primary stellar surface and see if they can explain the formation of a bipolar nebula. To do so, we compute the first binary models of AGB

stars allowed to be spun-up by tidal interactions, and study which rotational velocity we can get using this approach. As we mentioned in paper I, surface rotational velocity values above 2 km s^{-1} could in principle produce considerable asymmetries in these stars.

The spin-up of stellar envelopes has only been calculated for massive stars (see Detmers et al. 2008) to explain the formation of gamma-ray bursts. We recall however that although the present calculations are the first in the context of the formation of bipolar PNe, the idea has been around for quite some time. Livio (1994) first mentioned tidal spin-up as a possible origin of bipolar PNe and later on Soker (1998) suggested that as a consequence of the spin-up, the primary's envelope could rotate at several percent of the breakup velocity, and this will probably result in a small, but non-negligible, effect on the mass-loss geometry. In this paper we precisely focus on above ideas, and compute how important spin-up is in this context. The outline of the paper is as follows: § 2 describes the numerical scheme and physical approximations as well as the inputs in our calculations; § 3 shows the results of the stellar evolution calculations; and finally in § 4 we disscus the results and provide the main conclusions of this study.

2. STELLAR MODELS, METHODS AND PHYSICAL ASSUMPTIONS

The stellar evolution calculations have been done using the Binary Evolution Code (BEC) (Petrovic et al. 2005; Yoon et al. 2006). BEC is a one-dimensional hydrodynamic, stellar evolution code designed to evolve stellar models of single and binary stars, which originates from the STERN code (Langer 1991). The structure and evolution of stars is governed by a set of partial differential equations, the so-called stellar structure equations. In BEC, which uses the hydrodynamic version, the inertia terms are used (see Kozyreva et al. 2014). This code includes diffusive mixing due to convection, semi-convection (Langer et al. 1985), and thermohaline mixing as in Wellstein et al. (2001) and Cantiello & Langer

(2010) .

In rotating stars, centrifugal forces act on the stellar gas leading to deviations from spherical symmetry. For slow to moderate rotation these deformations remain rotationally symmetric (Tassoul 1978), and no triaxial deformations are expected. The shapes of equipotentail surfaces are affected by the centrifugal potential and therefore deviate from spherical symmetry. In this scenario, the momentum equation and the energy transport equation for spherical symmetric stars have to be modified. To take this effect into account, the effect of the centrifugal force on the stellar structure is calculated following the method of Kippenhahn & Thomas (1970) in the approximation of Endal & Sofia (1976), and applied to the hydrodynamic stellar structure equations (Heger et al. 2000). Thus, instead of spherical shells, the mass shells correspond to surfaces of constant pressure. The corrections are applied to the acceleration and the radiative temperature gradient. According to Zahn (1975), Chaboyer & Zahn (1992) and Zhan (1992), anisotropic turbulence acts much stronger on isobars than in perpendicular directions. This enforces shellular rotation rather than cylindrical rotation, and it removes compositional differences on isobaric surfaces. Therefore, it can be assumed that the matter on such surfaces is chemically homogeneous. Together with the shellular rotation, this allows to retain the one-dimensional approximation (Heger et al. 2000).

Time-dependent chemical mixing and transport of angular momentum due to rotationally-induced instabilities, including the shear instability and the Golreich-Schubert-Fricke instability, and the Eddington-Sweet circulations are also included as a diffusive process (Heger et al. 2000). We also include the transport of angular momentum due to magnetic fields (Spruit 2002), as in Heger et al. (2005) and Petrovic et al. (2005). They considered dynamo action in radiative layers, resulting from winding up magnetic fields due to differential rotation, that creates toroidal fields, and generation of poloidal

fields from toroidal fields due to the Tayler instability (the Talyer-Spruit dynamo). The strength of magnetic fields is calculated using the steady state solution of the Tayler-Spruit dynamo, which is given as a function of the degree of differential rotation. The magnetic field therefore is instantaneous and has no memory of previous timesteps. In our cases, the strongest magnetic field is found in the boundary layer between the core and the envelope where the degree of differential rotation is the largest, while in the rest of the envelope, magnetic fields are very weak. The rotation profile in the convection zone is self-consistently calculated by solving the diffusion equation for the transport of angular momentum.

The physics of binary interactions was implemented by Braun (1997, PhD Thesis) and Wellstein (2001, PhD Thesis). We assume a circular orbit and adopt the Eggelton's approximation for the Roche-lobe radius (Eggelton 1983), for our considered binary systems. We calculate the mass transfer rate due to Roche-lobe overflow following the method by Ritter (1988), in an implicit way (Note, however, that our models do not involve mass transfer in this article). We adopt the prescription by Podsiadlowski et al. (1992) to calculate the evolution of the binary orbit resulting from mass transfer and stellar winds mass loss, and the numerical result by Brooksaw and Tavani (1993) to calculate the amount of specific angular momentum of the stellar wind material that escapes the binary system.

The synchronisation of the binary system is computed with the same method as in Wellstein (2001) (see also Detmers et al. 2008), using the synchronisation time given by Zahn (1977) for convective stars :

$$\tau_{\rm sync} \propto q^{-2} \left(\frac{d}{R}\right)^6 , \qquad (1)$$

where $q = M_2/M_1$ is the mass ratio of the binary, with M_1 the mass of the primary star that evolves up to the AGB phase, and M_2 the mass of the secondary main sequence star, d is the orbital separation, and R the radius of the primary AGB star. The angular momentum exchange ΔJ that is added to the whole AGB star at each time step Δt due to

tides is

$$\Delta J \ = (J_{\rm AGB} - J_{\rm sync}) \left(1 - {\rm e}^{-\Delta t/\tau_{\rm sync}}\right) \ , \tag{2}$$

where $J_{\rm sync}$ is the spin angular momentum that the AGB star would have when the system is in synchronous rotation.

Recently, Paxton et al. (2015) implemented binary physics into the MESA code, by including many ingredients from BEC. Since the two codes use very similar physics, a comparison of the two would not be too meaningful (see Section 2.6 for Numerical Tests in Paxton et al. 2015). There exists no other code that includes both binarity and differential rotation at the present. The accuracy of our results is more dependant on the synchronization physics rather than on numerics, because the numerical implementation is quite straightforward. Along these lines, there two articles which are useful to mention. In the first one, Khaliullin & Khaliullina (2010) found that Zahn's theory is consistent with observations of 101 eclipsing binaries with early-type main-sequence component, and in the second one, Zamanov et al. (2007) reports evidence for synchronisation of 29 S-type symbiotic stars, which are similar type of binaries. The assumption of circular orbits is a good approximation in our case, since the circularization timescale is comparable to synchronization timescale. In the case that the orbits were very eccentric, there might be episodes of mass transfer when the stellar components become close enough, for a given mean orbital separation. Considering such a situation would be very interesting, but will be the subject of future work (see Staff et al. 2015 for a recent work along these lines).

The majority of Solar-type stars did seem to have stellar companions (Abt & Levy 1976; Duquennoy & Mayor 1991). The fraction of main sequence binaries was found to be in the range from 65 % to 100 % with only about 30% G-dwarf primaries having no companion up to about 0.01 $M_\odot$ (Duquennoy & Mayor 1991). The multiplicity fraction however seems to have a dependency on the mass of the primary with binary systems being

about 50 % between spectral types B4 and A7 (Kouwenhoven et al. 2007) and about 33 % for F6-K3 stars using the more recent estimates by Raghavan et al. (2010). These values are consistent with the fraction of binary systems found in central stars of PNe (Douchin et al. 2015). Note that both the binary period distribution and the binary fraction are meaningful in doing this comparison.

In the current study, we use binary systems where the primary star have an initial mass of 2.5 $M_{\odot}$. The main reason that motivate the choice of the initial progenitor mass is the higher mass stellar progenitor that the bipolar PNe morphological class seem to have, as indicated by their chemical abundances (see e.g. Stanghellini et al. 2006; Manchado 2004), and their closer distribution to the galactic plane (Calvet & Peimbert 1983; Corradi & Schwarz 1995, Manchado 2004; see also paper I García-Segura et al. 2014). For the binary system, we have chosen as the secondary a stellar companion with 0.8 $M_{\odot}$. These stars represent one of the most numerous stars on the main sequence and have been found to be numerous as well as secondaries in the study of Sco OB2 by Kouwenhoven et al. (2005). A mass fraction $q = M_2/M_1$ of 0.32 seems to be reasonably likely and consistent with the observed values by Kouwenhoven et al. (2005). Note that Duquennoy & Mayor (1991) also found that the binary mass distribution peaks around $q = 0.3$ for Solar-type stars concluding that in general binaries can be formed by association of stars build from the same IMF. The secondary star is treated as a point mass in this study.

For the stellar mass-loss rate we adopted Reimers (1975) with $\eta = 0.5$ during the Red Giant phase and the Vassiliadis & Wood (1993) parameterization for the AGB phase.

We have computed two sets of models (8 in total) from the zero age main sequence (ZAMS) to the AGB phase using primaries with two different initial stellar rotation rates and four different binary initial orbital separations. The binary parameters of all the computed models at the ZAMS are listed in Table 1. In the first set of models we consider

a very small initial rotation, nearly zero, which is the rotation that would result from synchronization at the zero age main sequence (ZAMS). For the second set of models we have adopted an initial equatorial rotation velocity of 250 km s^{-1} at the ZAMS representative of single stars (Fukuda 1982) with the mass of the primary. This velocity has been chosen as well to allow comparisons with the results from paper I. The initial orbital separations used in the calculations are 5, 6, 7 and 8 AU. To make the choice for the separations of the binaries, we computed first preliminary basic models that allowed us to select two cases with RLOF and two cases that avoid RLOF, as it will be discussed in the next section. The minimum binary separation of 5 AU has been tuned to ensure that binary interaction is achieved during the late AGB phase, avoiding altogether a strong tidal interaction during both the main sequence and the Red Giant Branch phase.

3. RESULTS

The evolution of the surface equatorial rotational velocity during the thermal pulsing AGB phase is shown in Figure 1, for each of the initial binary parameters listed in Table 1. We do not show the earlier evolution because the tidal spin-up is not important as the synchronization time is quite dependent of the radius (see equation 1). Only when the stellar radius during the AGB is large enough, for a given binary separation, tidal forces become important and the synchronization time is short enough that the spin-up becomes evident. Figure 1 also shows for comparison (dotted line) the results of the model presented in paper I in which we included angular momentum transport induced by magnetic torques inside the star.

We see in Figure 1 that all the binary models have larger surface rotational velocities than the single stellar models computed in paper I (where surface rotational velocities larger than 1 km s^{-1} were never reached at the late thermal pulsing AGB phase). We find that

the models with initial separations of 5 and 6 AU end up in RLOF phases while the models with initial separations of 7 and 8 AU avoid RLOF altogether. The AGB stars, in the more separated binary models, reach moderate rotational velocities at the surface (~ 3.5 and ~ 2 km s^{-1} for models with 7 and 8 AU respectively) during the inter-pulse phase, just before the last two thermal pulses, and for the closest binary separations explored, 5 and 6 AU, the AGB stars reach rotational velocities of ~ 6 and ~ 4 km s^{-1} respectively, when the RLOF is initiated. Note that the models that do not enter in the RLOF phase lose most of the gained angular momentum via the wind during the last two thermal pulses. This is clearly reflected in Figure 1 with the quick drop of velocity at the end of their AGB evolution.

We find that the maximum rotation velocity gained at the thermal pulsing AGB phase does not depend of the initial velocity assumed for the primary, but only on the initial separation of the binary. To illustrate this we plot the spin angular momentum of the primary star in Figure 2. We find that the final spin angular momentum reached by the star is independent of the initial assumption, since the major contribution to the spin angular momentum of the primary comes from the orbital angular momentum. Although there is an important transfer of orbital angular momentum to the primary spin angular momentum, the separation (and the orbital period) growth in time due to mass-loss, as it is seen in Figure 3. This figure also shows that models c5 and r5 have almost reach corotation at the time our computation is stopped (because they reach RLOF). Models c6 and r6 are slightly below the corotation speed.

One of the most important results of the comparison allowed by our models is that the binaries that do not reach RLOF lose the gained angular momentum by mass-loss at the end of the AGB phase. This means that for these models the formation of bipolar nebulae via magnetohydrodynamical collimation is not possible, since at the time when a PN is formed, after an uncertain amount of transition time, the stellar surface rotation is very

small, and the effect that the secondary might have had in speeding up the primary will be negligible due to the large separation. Since the sound speed at the surface of an AGB star is of the order of ≈ 1 km s^{-1}, values below that for the rotation will not have any impact on the wind compression mechanism (Bjorkman & Cassinelli 1993; Ignace et al. 1996). When the calculations are stopped, we obtain surface rotational speeds of 0.03, 0.03, 0.4 and 0.09 km s^{-1} for models c7, c8 , r7 and r8 respectively. The stellar parameters are shown in Table 2.

On the other hand, the models that reach RLOF generate, for a timespan that requires further calculations, the necessary dynamical conditions to form an equatorial density enhancement in the circumbinary medium, since the rotation is fast (~ 6 km s^{-1}) and most likely sustained for the necessary time. These models are promising in forming bipolar nebulae as we will discuss in the next section. Table 3 gives the parameters of the binary systems approaching the RLOF phases at the time the computations are stopped.

4. DISCUSSION AND CONCLUSIONS

Our set of binary calculations shows that it seems a very reasonable assumption that the models that avoid RLOF phases will not form bipolar PNe, since all the gained angular momentum during the AGB phase will be lost via the wind in the last two thermal pulses. It is important to note as well the fact that the whole timescale affected by this process is very long, of the order of 100,000 yr, taking into account the last thermal pulse, and the possibility of a few thousand years more of uncertain transition time until the central star is hot enough for the fast wind mechanism to operate and shape the nebula (see e.g. Villaver et al. 2002). Any fingerprint of a transient, equatorial density enhancement will be dissipated at the time of PN formation in these models. Then, only the models that reach the RLOF phases are promising to explore bipolar PNe shaping, since their evolution will

proceed differently than those for single stars or non-contact binaries.

Following our results, it will be extremely useful to have the distribution and latitudinal dependence of the stellar wind coming out from the binary system, in order to model the formation of a bipolar PNe. Unfortunately, the equations by Bjorkman & Cassinelli (1993) and Ignace et al.(1996) that study the formation of wind-compression zones and wind-compression disks around single stars cannot be applied directly in this case, since the geometry is different for binary systems and the center of mass of the binary is not at the center of the AGB star. Currently, there is not any analytical or semi-analytical study that predict the distribution of gas in the nearby circumbinary medium for these binary stars, except for the studies where the outflow comes from the Lagrange point L_2 (Shu et al. 1979), as we will discuss below.

We have made a rough estimate on how important a wind compression mechanism could be using the results of our models and keeping in mind the applicability restrictions outlined above. We focus the discussion in the last output from model c5. In this model the AGB star is at 19 % of its critical rotation speed, which according to Ignace et al.(1996) can be translated into a density contrast ratio equator/pole of ~ 9. Note that these numbers are given in the non-inertial reference frame of the AGB star but we can translate them to the inertial, reference frame at the center of mass. The total mass of the binary system is 3.006 $M_\odot$ (accounting for the mass lost) and the center of mass is located at 306 $R_\odot$ from the center of the AGB star, i.e., $\sim$ 26 % inside of its envelope. With this is mind, the equatorial surface at the opposite side of the secondary has a velocity of 14 km s^{-1} , which translates into close to $\sim$ 50 % of the critical rotation at that location. A 50 % of the critical rotation is within the range of conditions for the wind-compression disk formation, of course if the equations of Ignace et al.(1996) could be applied in the scenario we have just described. What this exercise emphasizes is that mass-loss is expected to be important

at the opposite side from the secondary, in the direction of the Lagrange point L_3, where the escape velocity at the surface is smaller than the value that an isolated star would have. This mass-loss enhancement is expected to occur with the shape of a spiral arm.

It is also important to mention that the system will lose an important amount of mass through the Lagrange point L_2. This mass-loss is expected to have the shape of a spiral arm as well, since the mass ratio q = 0.36 at the beginning of the RLOF phase is inside the range $0.064 \leq q \leq 0.78$ (see e.g. Shu et al. 1979; Mohamed & Podsiadlowski 2012; Pejcha et al. 2015). It is also interesting to note in this context that the ratio q increases along the subsequent evolution as the primary looses mass and the secondary accretes part of it. Once that the ratio q exceeds the value of 0.78, and if the system is still in RLOF, the ejection of gas through L_2 will piles up at a finite radius and will form a bounded mass-loss ring instead of an unbound outflow (Shu et al. 1979).

How much time the system will remain in the RLOF phase depends on the rate at which the AGB radius expands, how soon the common envelope is formed, the rate at which orbital angular momentum is lost (shrinking the orbit of the binary system) and on the mass-loss rate from the binary system (increasing the orbital distance). In any case, the proper computations of the mass-loss through the Langrangians points L_2 and L_3 is challenging. These new scenarios are of great interest for future hydrodynamical computations for the formation of bipolar PNe such as the ones recently carried out by Staff et al. (2015).

From our binary stellar evolutionary models with an initial q = 0.32, we find that the maximum rotation velocity during the AGB phase, as a result of tidal spin-up, is independent of the initial rotational velocity at the ZAMS, and only depends on the initial separation.

We find very unlikely that binaries which avoid the RLOF phases could form bipolar

PNe with an equatorial waist. The angular momentum lost by the stellar winds in the last thermal pulses, and the unknown transition time from the AGB to the PN formation will dissipate any transient, equatorial density enhancement formed in the nearby circumbinary medium. The same reasoning applies to the engulfment of giant planets if they do not produce the ejection of the envelope, since no matter how much angular momentum is gained by the AGB star, the last thermal pulses will carry it away via the stellar winds.

The above discussion is focussed only in the classical formation of bipolar nebulae, in which a slow, equatorially denser wind inhibits the future expansion of a fast wind in the equatorial regions. However, this is not the only model that accounts for the formation of bipolarity, since jets and collimated outflows may form around the companion (Soker & Rappaport 2000; Huarte-Espinosa et al. 2013) and power PNe, as they are known to do in Symbiotics (Corradi & Schwarz 1993). These scenarios are based on the formation of an accretion disk around the secondary star, where the ejected collimated gas forms the bipolar nebula, before the formation of a fast wind by the central star. The separation of the binary system is crucial here in determining the energy of the outflow. According to the separation of the binary, the systems can be classified into three types: Wind-Capture disks for large separations; Wind-RLOF disks for small separations, but still larger than the distances required for RLOF; and the RLOF disks formed at the RLOF phases. Note that systems with small separations (such as models c5, c6, r5 and r6) will pass through the three different types consecutively, as the AGB radius increases during stellar evolution. In the Wind-Capture disk, a companion orbiting through the dense wind of an AGB star will capture enough wind material to form an accretion disk and (most likely) power a jet (Huarte-Espinosa et al. 2013). The Wind-RLOF disk is a relatively new mechanism which allows far larger orbital separations than traditional RLOF. High accretion rates are possible with Wind-RLOF scenarios and the determination of its presence requires solutions for the AGB wind structure (Podsiadlowski & Mohamed 2007; Mohamed & Podsiadlowski

2012). Finally, we have the outflows from RLOF phases, where the amount of accretion is the largest one. Although neither of these possibilities are accounted for in the present study, they are not exclusive, in the sense that the three types, specially the last two (Wind-RLOF and RLOF) will form also a density enhancement in the orbital plane with a spiral shape, due to the mass-loss through the Lagrange point L_2. In other words, the accretion disks will form both the jets and the density enhancement in the orbital plane.

Since the orbital separation increases very fast at the last thermal pulses due to the large mass-loss (Figure 3), the wind accretion is expected to decay with time in the first two scenarios. Thus, it is very likely that the formation of bipolar PNe follows the evolution of binary systems with separations where RLOF phases are attained, as well as the subsequent (or imminent) common envelope phases. Proper computations of the time spent in each of the three phases will be extremely important and will be the subject of future studies.

Finally, another point which needs consideration in this study is the role of magnetic fields. The creation of fields by companions in common envelope scenarios has been discussed in the literature and offers another route whereby binary stars produce bipolar PNe (Tout & Regös 2003; Nordhaus & Blackman 2006). Note that the spin-up of the envelope in the above studies is the direct product of a spiral-in process during the common envelope evolution. In our cases, however, the spin-up of the envelope is due to tidal forces. In the case of non-contact binaries, we found that magnetic fields are very weak inside of the envelope where the degree of differential rotation is negligible. The rotation velocity become too small at the end of the AGB phase, and it would not make any big difference from single stars. We find very unlikely that magnetic fields could be of any importance here, which probably will have only a role in forming cool spots (Frank 1995; Soker 2001).

On the other hand, for the closest systems, it would make a big difference. Since AGB stars rotate at $\sim$ 20–50 % of their critical rotation, this is significant enough to make an

alpha-omega dynamo efficient. But, as we discussed above, they will become a common envelope soon once mass transfer starts, and the later evolution would be governed by common envelope. So, probably, even in this case, the role of convective dynamo might be minor, although this requires further investigation, since the accumulate magnetic energy could be important for the ejection of the envelope.

In conclusion, this study rules out that tidal spin-up in non-contact binaries could be a sufficient condition to form bipolar PNe.

G.G.-S. is partially supported by CONACyT grant 178253. E.V. and A.M. work was supported by the Spanish Ministry of Economy and Competitiveness, Plan Nacional de Astronomía y Astrofísica, under grants AYA2014-55840-P and AYA-2011-27754 respectively. We would like to thank our anonymous referee for his valuable comments which improved the presentation of the paper.

REFERENCES

Abt, H. A., & Levy, S. G. 1976, ApJS, 30, 273

Balick, B. 1987, AJ, 94, 671

Bjorkman, J. E. & Cassinelli, J. P. 1993, ApJ, 409, 429

Braun, H. 1997, PhD Thesis, Ludwig-Maximilians Universtaet, Munich

Braun, H. & Langer, N. 1995, in IAU Symposium 163, 305

Brookshaw, L., & Tavani, M. 1993, ApJ, 410, 719

Calvet, N., & Peimbert, M. 1983, RMA&A, 5, 319

Cantiello, M., Langer, N. 2010, A&A, 521 , 9

Corradi, R. L. M. & Schwarz, H. E. 1993, A&A, 268, 714

Corradi, R. L. M. & Schwarz, H. E. 1995, A&A, 293, 871

Chevalier, R. A., & Luo, D. 1994, ApJ, 421, 225

De Marco, O. 2009, PASP, 121, 316

De Marco, O., Passy, J.-C., Frew, D. J., Moe, M., Jacoby, G. H. 2013, MNRAS, 428, 2118

Detmers, R. G., Langer, N., Podsiadlowski, Ph., and Izzard, R. G. 2008, A&A, 484, 831

Douchin, D., De Marco, O., Frew, D. J., et al. 2015, MNRAS, 448, 3132

Duquennoy, A., & Mayor, M. 1991, A&A, 248, 485

Eggleton, P. 1983, ApJ, 263, 368

Endal, A., & Sofia, S. 1976, ApJ, 210, 184

Frank, A. 1995, AJ, 110, 2457

Frank, A. & Mellema, G. 1994, A&A, 289, 937

Fukuda, I. 1982, PASP, 94, 271

García-Segura, G., Villaver, E., Langer, N., Yoon, S.-C., & Manchado, A. 2014, ApJ, 783, 74, paper I

Gawryszczak, A. J., Mikolajewska, J., & Różyczka, M. 2002, A&A, 385, 205

García-Segura, G. 1997, ApJ, 489, L189

García-Segura, G., Langer, N., Różyczka, M., & Franco, J. 1999, ApJ, 517, 767

Heger, A., Langer, N., & Woosley, S. E. 2000, A&A, 2000, ApJ, 528, 368

Heger, A., Woosley, S. E., & Spruit, H. C. 2005, ApJ, 626, 350

Huarte-Espinosa, M., Carroll-Nellenback, J., Nordhaus, J., Frank, A., & Blackman, E. G. 2013, MNRAS, 433, 295

Icke, V. 1988, A&A, 202, 177

Icke, V., Preston, H. L. & Balick, B. 1989, AJ, 97, 462

Ignace, R., Cassinelli, J. P., & Bjorkman, J. E. 1996, ApJ, 459, 671

Khaliullin, Kh. F., & Khaliullina, A. I. 2010 , MNRAS, 401 , 257

Kouwenhoven, M. B. N., Brown, A. G. A., Portegies Zwart, S. F., & Kaper, L. 2007, A&A, 474, 77

Kouwenhoven, M. B. N., Brown, A. G. A., Zinnecker, H., Kaper, L., & Portegies Zwart, S. F. 2005, A&A, 430, 137

Kozyreva, A., Yoon, S.-C., Langer, N. 2014, A&A, 566, 146

Lamers, H. J. G. L. M., & Fitzpatrick, E. L., 1988, ApJ, 324 , 279

Langer, N. 1991, A&A, 252, 669

Langer, N., El Eid, M. F., & Fricke, K. J. 1985, A&A, 145, 179

Livio, M. 1994, in Circumstellar Media in Late Stages of Stellar Evolution, ed. R Clegg, P. Meikle, & I. Stevens (Cambridge: Cambridge Uni. Press), 35

Livio, M. 1993, in IAU Symp. No 155 "Planetary Nebulae", ed. R. Weinberger and A. Acker, (Kluwer Academic Publishers, Dordrecht), 279

Manchado, A., Villaver, E., Stanghellini, L., & Guerrero, M. A. 2000, ASP Conference Series, 199, 17

Matt, S., Balick, B., Winglee, R., & Goodson, A. 2000, ApJ, 545, 965

Mellema, G., Eulderink, F. & Icke, V. 1991, A&A, 252, 718

Mohamed ,S., & Podsiadlowski, Ph. 2012, Baltic Astronomy, 21, 88

Nordhaus, J., & Blackman, E. G. 2006, MNRAS, 370, 2004

Passy, J.-C., De Marco, O., Fryer, C. L., Herwig, F., Diehl, S., Oishi, J. S., Mac Low, M.-M., Bryan, G. L., & Rockefeller, G. 2012, ApJ, 744, 52

Paxton, B., Marchant, P., Schwab, J., et al. 2015, ApJS, 220, 15

Pejcha, O., Metzger, B. D., & Tomida, K. 2015, MNRAS, in press

Petrovic, J., Langer, N., Yoon, S.-C., & Heger, A. 2005, A&A, 435, 247

Podsiadlowski, Ph., Joss, P. C., & Hsu, J. J. L. 1992, ApJ, 391, 246

Podsiadlowski, Ph., & Mohamed, S. 2007, Baltic Astronomy, 16, 26

Raghavan, D., McAlister, H. A., Henry, T. J., Latham, D. W., Marcy, G. W., Mason, B. D., Gies, D. R., White, R. J., & ten Brummelaar, T. A. 2010, ApJS, 190, 1

Reimers, D. 1975, Mem. Soc. Liege, 8, 369

Ricker, P. M., & Taam, R. E. 2012, ApJ, 746, 74

Ritter, H. 1988, A&A, 202, 93

Sandquist, E. L., Taam, R. E., Chen, X., Bodenheimer, P., & Burkert, A. 1998, ApJ, 500, 909

Shu, F. M., Anderson, L., & Lubow, S. M. 1979, ApJ, 229, 223

Skopal, A., & Cariková, Z. 2014, eprint arXiv:1410.7674

Soker, N. 1997, ApJS, 112, 487

Soker, N. 1998, ApJ, 496, 833

Soker, N. 2001, MNRAS, 324, 699

Spruit, H. C. 2002, A&A, 381, 923

Staff, J. E., De Marco, O., Macdonald, D., Galaviz, P., Passy, J.-C., Iaconi, R., & Mac Low, M.-M. 2015, in press

Stanghellini, L., Guerrero, M. A., Cuuha, K., Manchado, A., & Villaver, E. 2006, ApJ, 651, 898

Tassoul, J.-L. 1978, *Theory of Rotating Stars*, Princeton Univ. Press, Princeton.

Tout, C. A. & Regös, E. 2003, ASP Conference Series, 293, 2003

Vassiliadis, E., & Wood, P. R. 1993, ApJ, 413, 641

Villaver, E., Manchado, A., & Garc¡92¿a-Segura, G. 2002, ApJ, 581, 1204

Wellstein, S., Langer, N., & Braun, H. 2001, A&A, 369, 939

Wellstein, S. 2001, PhD Thesis, University of Postdam

Yoon, S.-C., Langer, N., & Norman, C. 2006, A&A, 460, 199

Zamanov, R. K., Bode, M. F., Melo, C. H. F., Bachev, R., Gomboc, A., Stateva, I. K., Porter, J. M., Pritchard, J. 2007 , MNRAS, 380, 1053

This manuscript was prepared with the AAS LaTeX macros v5.2.

Table 1: Initial Parameters of Binary Stellar Models at ZAMS

Model	d (A.U.)	M_1 ($M_\odot$)	M_2 ($M_\odot$)	$v_{\rm rot}$ (km s^{-1})	Description
c5	5	2.5	0.8	~ 0	corotation
c6	6	2.5	0.8	~ 0	corotation
c7	7	2.5	0.8	~ 0	corotation
c8	8	2.5	0.8	~ 0	corotation
r5	5	2.5	0.8	250	fast rotator
r6	6	2.5	0.8	250	fast rotator
r7	7	2.5	0.8	250	fast rotator
r8	8	2.5	0.8	250	fast rotator

Table 2: Primary Stellar Parameters at the End of Computations

Model	M ($M_\odot$)	$logL$ ($L_\odot$)	$T_{\rm eff}$	R ($R_\odot$)	$< v_{\rm rot} >$ (km s^{-1})	$P_{\rm orbital}$ (d)
c7	0.819	4.134	2970	441	0.03	11949
c8	0.836	4.188	3148	417	0.03	15164
r7	0.841	4.212	3164	424	0.44	11601
r8	0.816	4.265	3159	452	0.09	15631

Table 3: Primary Stellar Parameters when Roche Lobe Overflow is approached

Model	M ($M_\odot$)	$logL$ ($L_\odot$)	$T_{\rm eff}$	R ($R_\odot$)	$< v_{\rm rot} >$ (km s^{-1})	d ($R_\odot$)	$P_{\rm orbital}$ (d)
c5	2.206	4.147	3076	415	6.1	1151.53	2612.62
c6	1.869	4.226	2887	518	4.9	1480.16	4040.97
r5	2.239	4.149	3086	415	5.8	1144.73	2575.88
r6	1.999	4.239	2923	513	4.8	1443.27	3799.25

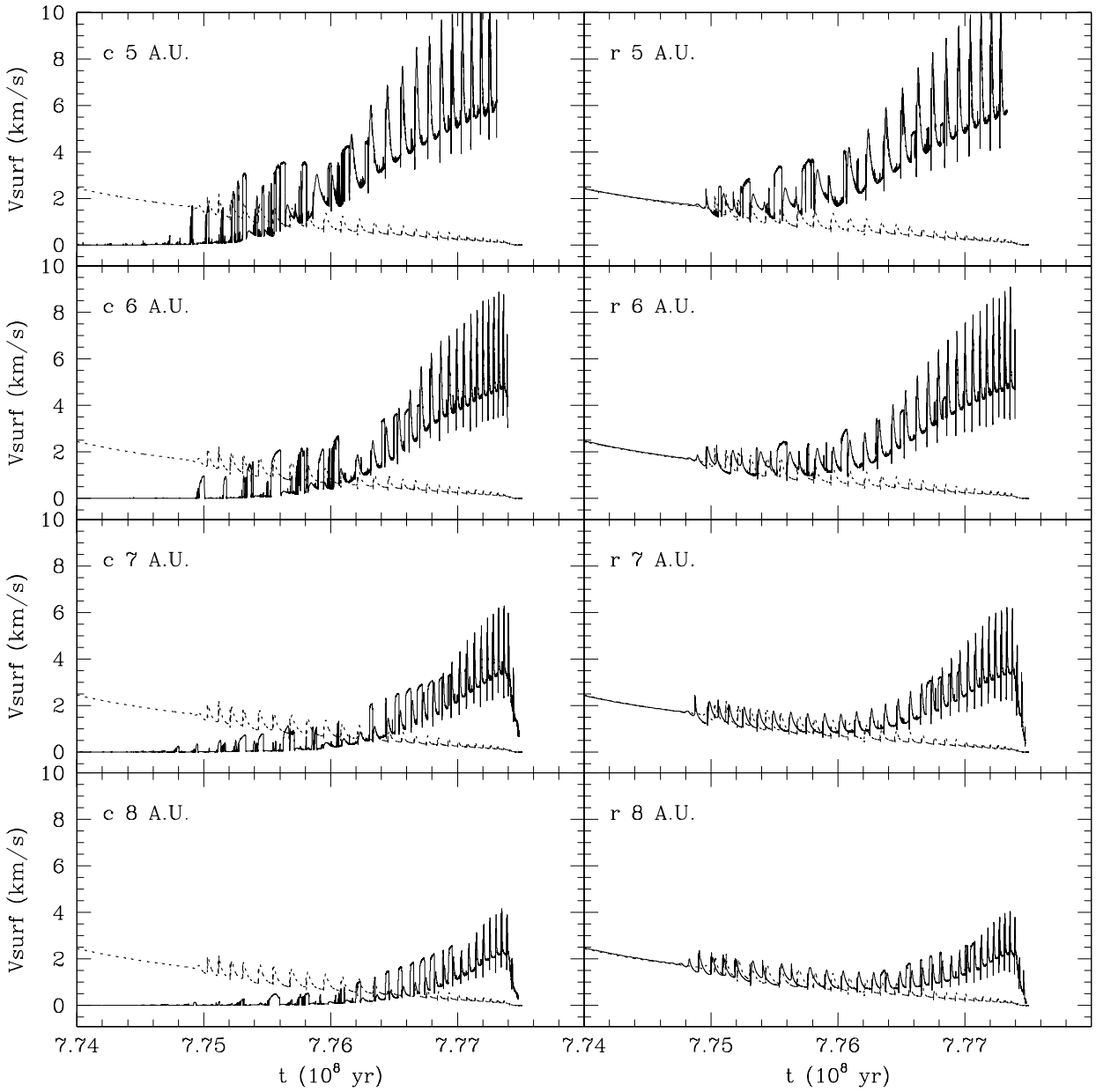

Fig. 1.— Evolution of the surface equatorial rotational velocity during the thermal pulsing AGB phase. Left: models with ZAMS velocities nearly zero, c5, c6, c7 and c8. Right: models with ZAMS velocities of 250 km s^{-1} , r5, r6, r7 and r8. The initial binary separation is labeled in the upper left corner. The dotted lines correspond to the magnetic model of paper I as a reference.

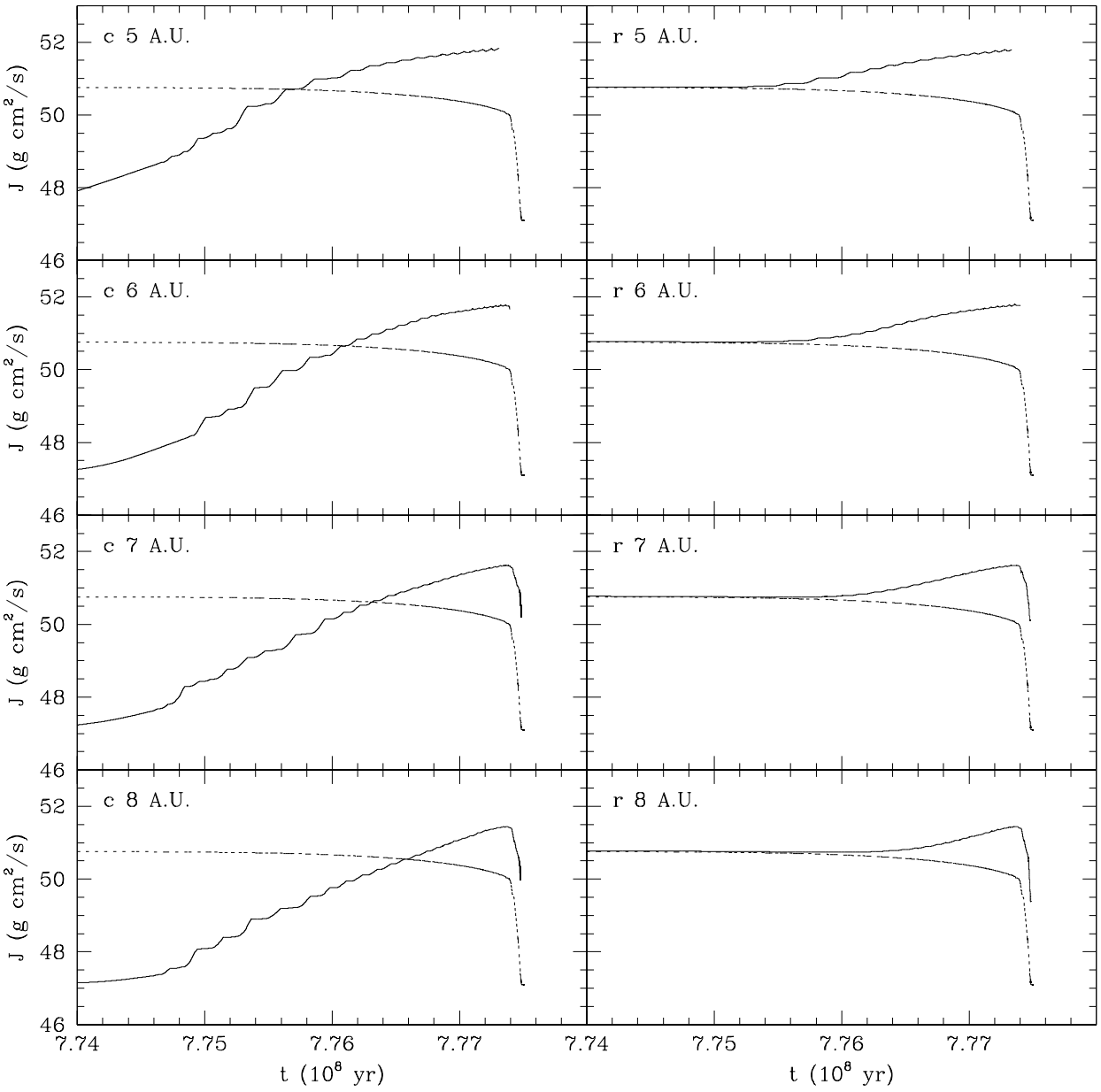

Fig. 2.— Same as figure 1 for the evolution of the spin angular momentum

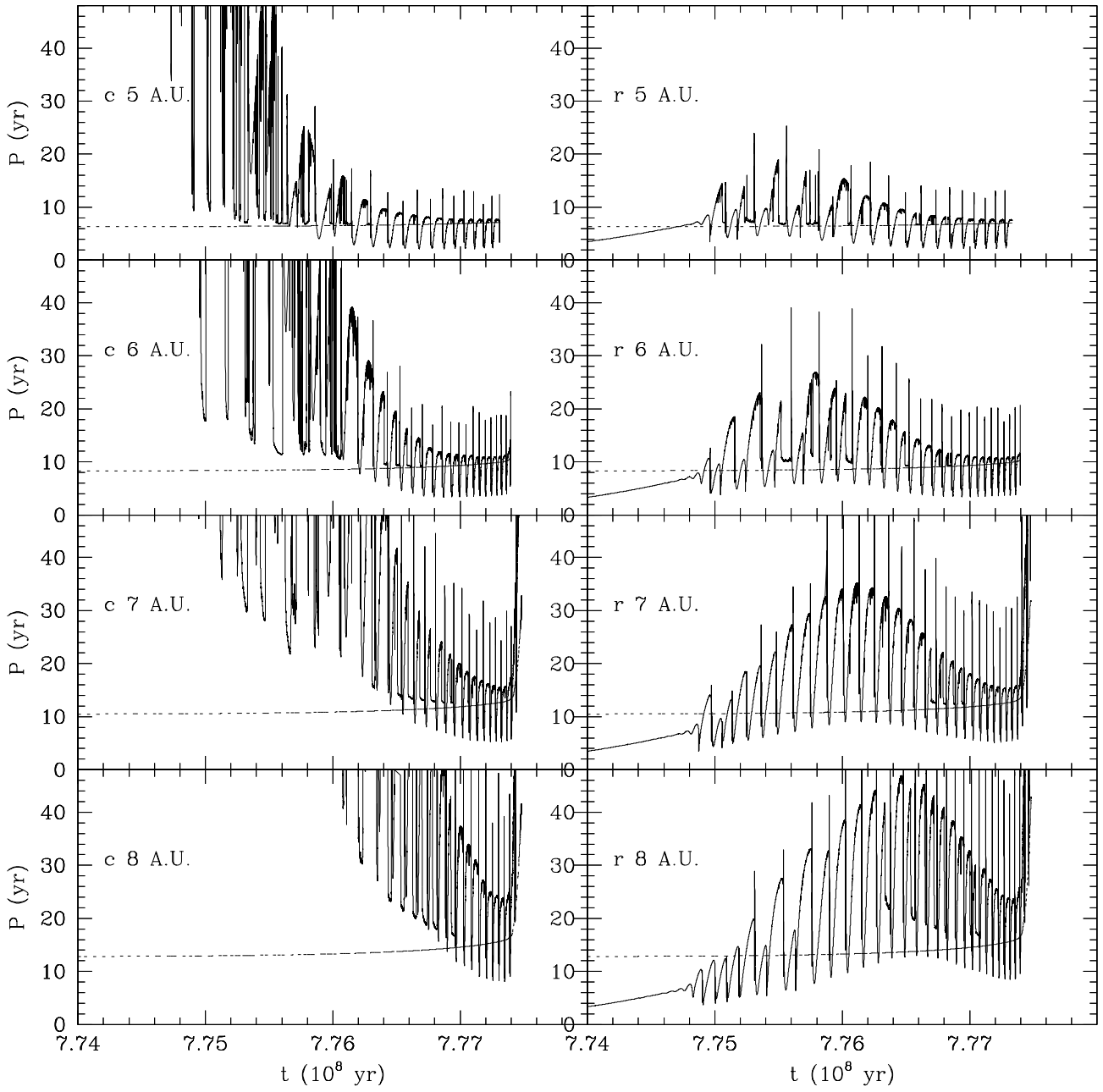

Fig. 3.— Evolution of the spin period (solid line) and orbital period (dotted line) during the thermal pulsing AGB phase for models c5, c6, c7 and c8 (left panels) and models r5, r6, r7 and r8 (right).